

Investigation of Antibacterial Coatings Based on Chitosan/Polyacrylic Acid/Chlorhexidine for Orthopedic Implants

Balzhan Savdenbekova,* Ayazhan Seidulayeva, Aruzhan Sailau, Zhanar Bekissanova, Dilafuz Rakhmatullayeva, and Ardak Jumagazyeva

Cite This: *ACS Polym. Au* 2024, 4, 498–511

Read Online

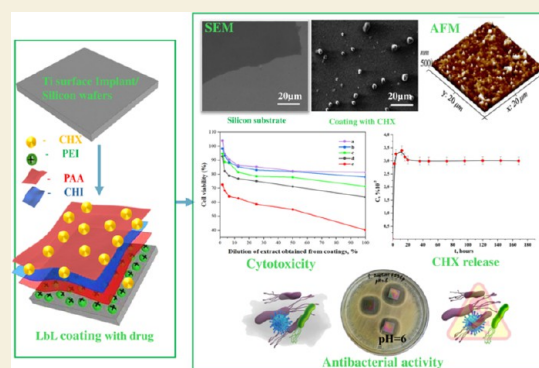
ACCESS |

Metrics & More

Article Recommendations

ABSTRACT: Antibacterial coatings on model silicon wafers and implants, based on chitosan (CHI), poly(acrylic acid) (PAA), and the antibacterial agent chlorhexidine digluconate (CHX), were obtained using a layer-by-layer assembly method. The surface roughness and 2D and 3D images of the surfaces of CHI/PAA/CHX coatings obtained from different pH assemblies were investigated by atomic force microscopy, revealing that pH 6 enabled optimal inclusion of CHX in the multilayer film. The structure and elemental composition before and after implementation of CHX into the coating were investigated via scanning electron microscopy and energy-dispersive X-ray spectroscopy. The obtained films exhibited antimicrobial efficacy against *Staphylococcus aureus* and *Staphylococcus epidermidis*. The effects of CHX concentration and duration of contact with the coating on bacterial activity were investigated, and the quantitative release of CHX from coated implants in phosphate buffer was determined as a function of the incubation time. The biocompatibility of the PAA/CHI/CHX coatings was investigated using human mononuclear cells (HMNCs) and quantified using an MTT assay. HMNCs demonstrated high viability in eluted solutions obtained from implants coated with PAA/CHI/CHX (0.025%) and PAA/CHI/CHX (0.0125%), while the extract of implants coated with PAA/CHI/CHX (0.05%) induced slight cytotoxicity.

KEYWORDS: layer-by-layer assembly, antibacterial coating, chitosan, chlorhexidine, orthopedic implants



1. INTRODUCTION

Nowadays, stainless steel and titanium alloys are predominantly used as materials in permanent implants for orthopedic surgery due to their high corrosion resistance, mechanical strength, and biocompatibility.^{1,2} The growth of microbial biofilms on the implant surface can lead to the development of implant-associated infections and require additional surgical interventions, which in turn has negative social and economic consequences.^{3–6} The main causes of infections with orthopedic implants are Gram-positive bacteria, such as *Staphylococcus aureus* and *Staphylococcus epidermidis*, while streptococci and enterococci are usually involved in later stages.^{7,8} The need to combat these types of infections has led to the search for new research strategies aimed at protecting biomaterials and increasing their efficacy. In addition, the modified surface must be “intelligent” and respond to even minimal bacterial loads. Multilayer, so-called “layer-by-layer” (LbL) coatings, developed by Decher et al.,⁹ have been shown to accomplish this task. This method effectively produces antibacterial coatings via sequential application of special building blocks.¹⁰ An important feature of this technology is the wide range of individual bilayers, facilitating convenient

customization of surface chemistry.^{11,12} This method makes it possible to work with different types of molecules, such as organic and inorganic compounds, based on a wide range of interactions (electrostatic, hydrogen bonds, biospecific interactions, metal coordination, etc.), endowing the surface with the necessary chemical and biological properties.

LbL coatings based on biocompatible polyelectrolytes represent an important class of materials due to their biofunctionality and rich resources. One of the most commonly used components for such coatings is chitosan (CHI), a biopolymer that contains primary amino groups in its structure and has a positive charge, with a $pK_a \approx 6.24$ in acidic environments.^{13,14} CHI is biocompatible and degradable by enzymes in the human body, and its products are nontoxic.^{15,16}

Received: May 15, 2024
Revised: August 5, 2024
Accepted: August 6, 2024
Published: August 22, 2024



Recently, adoption of the LbL method with CHI has been reported to obtain various materials, such as films/coatings, capsules, and fibers, as well as the use of these biomaterials as antimicrobials, in drug delivery, as dressings, and in tissue engineering.^{17,18} CHI, the only natural cationic polysaccharide, has also been used in combination with other compounds as a reservoir for the delivery of various drugs, including CHI/caffeic acid,¹⁹ CHI/polycaprolactone,²⁰ CHI/hyaluronic acid,^{21–23} and CHI/ β -cyclodextrin.²⁴ These results suggest that antibacterial films based on a combination of CHI with various bioactive compounds may prove to be successful tools in the fight against infectious consequences during implantation.

The results of such research suggest a new scientific strategy aimed at protecting and improving the effectiveness of antibacterial protection in implantable medical devices. Herein, poly(acrylic acid) (PAA) was utilized to create LbL coatings with CHI. PAA is a biocompatible and hydrophilic polymer that is favored for biomedical applications due to properties such as pH sensitivity, complexity, and mucoadhesiveness.²⁵

LbL coatings based on PAA/CHI have been considered as storage and delivery systems for various drugs, such as propranolol,^{26,27} ciprofloxacin,²⁸ and tobramycin.²⁹ In most cases, antibiotics have been employed in such drug delivery systems, as they are widely used in the treatment of polymicrobial infections. However, when working with antibiotics, their concentrations must be carefully monitored to prevent the emergence of bacterial resistance in the peri-implant area.^{30–32} Despite the regulation of drug dosage, this approach faces challenges due to increasing bacterial resistance to commonly used antibiotics,³³ making antibiotic therapy less effective.^{34,35} Therefore, the development of antimicrobial delivery systems without the use of antibiotics, for example, using antiseptics, such as chlorhexidine (CHX), may be one of the most effective ways to treat infectious diseases. Herein, CHX was selected as an antibacterial agent to obtain an active nanocoating. Chlorhexidine gluconate is the gold standard in the field of antiseptics. The optimum pH range to achieve a maximum antibacterial effect is between 5.0 and 7.0.³⁶ Depending on the concentration, the effect of CHX can be bactericidal or bacteriostatic, and CHX has a broad spectrum of activity against Gram-positive and Gram-negative bacteria.³⁷ The antimicrobial activity of CHX is based on increased permeability of the cell membrane and subsequent coagulation of macromolecules in the intracellular cytoplasm.³⁸ Due to its unique properties, CHX has been successfully incorporated into various types of coatings, e.g., poly(allylamine hydrochloride) (PAH)/PAA to prevent bacterial colonization of wounds under biological dressings,³⁹ poly-L-glutamic acid/poly-L-lysine to protect suture threads,⁴⁰ carboxymethylcellulose/CHI for suture materials made of polyethylene terephthalate and polyamide,⁴¹ and poly(4-styrene sulfonic acid) (PSS)/poly(diallyldimethylammonium chloride), PAA/PAH, and PSS/PAH for various biomedical applications, such as orthopedic and dental applications.⁴²

Currently, there are basically two methods employed to avoid biofilm formation and mitigate the consequences associated with this complication: “bacteria-repelling surfaces” and “active action (killing)”. The former method includes strategies such as superhydrophobic (i) and hydrophilic (ii) surfaces, while the latter method comprises strategies such as contact-based (iii) and release-based (iv) antibacterial surfaces.⁴³ Strategy (i) is known to inhibit the adhesion of

bacteria due to the high surface free energy,⁴⁴ while strategy (ii) reduces the adhesion force between the bacteria and the surface.^{45,46} However, these strategies are effective only in the initial stage of biofilm formation and do not lead to complete bacterial destruction. Moreover, strategy (iii) only kills bacteria on contact by creating a coating with a positive charge.^{47,48} An analysis of the above-mentioned strategies shows that strategy (iv) is the most effective against biofilm formation as it allows long-term^{49,50} and controlled release of antimicrobial agents from the coating when surfaces require particular long-term antimicrobial efficacy and minimization of bacterial growth.⁵¹ In addition, research interest in strategy (iv) has considerably increased in recent years.

Implants composed of various materials with different chemical natures and physical characteristics are frequently used in modern medicine.⁵² The orthopedic implant market is heading⁵³ toward minimizing the consequences of bacterial colonization on implants since traditional antibiotic therapy is not effective in the fight against biofilm formation on implants due to the manifestation of antibiotic resistance.^{54,55} In addition, the use of antibiotics calls into question the effectiveness of treatment, increases the duration of hospitalization and rehabilitation, and requires high financial costs for medical care.⁵⁶ Considering these factors, to ensure their biocompatibility and prevent the formation of bacterial biofilms on implant surfaces, antibacterial coatings need to be created that can effectively interact with the biological medium. However, despite promising research in this area, there remains an urgent need for research aimed at obtaining coatings on real implants that can be used in practical medicine.

Polyelectrolyte multilayers (PEMs) obtained with PAA and CHI can be used as drug delivery systems. Herein, the study findings demonstrate that the morphology of the coating surface plays a decisive role in the introduction of CHX into PEMs. Coatings containing CHX obtained at different pH assemblies were shown to exhibit different zones of inhibition (ZIs). The effectiveness of the coatings against bacterial activity depended on the CHX concentration used for impregnation and the time of contact of the coating with bacteria. Additionally, the release of CHX from coatings on implants was studied. The absence of cytotoxicity of such coatings was proven *in vitro*, which will enable further preliminary clinical trials *in vivo*.

2. MATERIALS AND METHODS

2.1. Materials

Silicon plates with an oxide layer ($d = 4$ in, $t = 500$ μm , $\rho = 0.001$ – 0.005 $\Omega\text{-cm}$, P-type, orientation = 100, SiO₂ layer thickness = 300 nm) and titanium implants (composition: 99.892% Ti and 0.108% Zr; size: 2.4×1.0 , 2.3×1.0 , and 2.1×0.8 cm², $R_a = 476 \pm 5.6$ nm; Stryker Corp., Kalamazoo, MI, USA) were used as substrates. The polyelectrolytes were low-molecular-weight CHI ($M_w = 50$ – 190 kDa, Sigma-Aldrich, St. Louis, MO, USA) and poly(acrylic acid) ($M_w = 1.8$ kDa, Sigma-Aldrich). The antibacterial agent was CHX (a commercial solution of 2% CHX digluconate). Polyethylenimine (PEI, linear, average $M_n = 10,000$, PDI ≤ 1.3), hydrogen peroxide (H₂O₂, 30%), hydrochloric acid (HCl, chemically pure), sulfuric acid (H₂SO₄, 98%), sodium hydroxide (NaOH, chemically pure), and glacial acetic acid (CH₃COOH, $\geq 99.5\%$) were purchased from Sigma-Aldrich. Phosphate-buffered saline (PBS, pH 7.413 ± 0.01) was purchased from Reagecon Diagnostics Ltd. (Clare, Ireland).

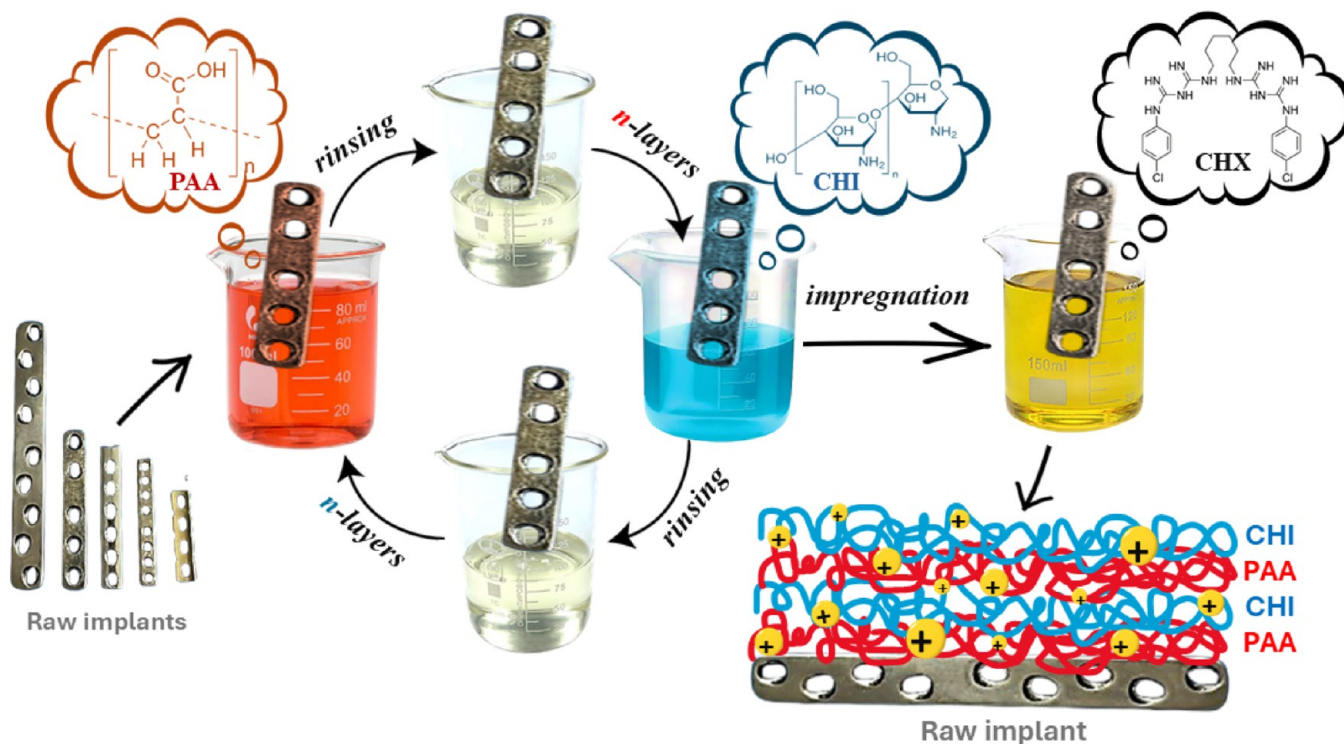


Figure 1. Scheme for obtaining PAA/CHI/CHX antibacterial coatings.

2.2. Pretreatment of Substrates

Silicon wafers were cut into plates of the same size ($1.5 \times 1.5 \text{ cm}^2$) using the TurboMarker system (IPG-Photonics, Oxford, MA, USA) in 10/20/30/50—a series of high-speed laser markings—based on a fiber laser with a pulsed ytterbium fiber laser. The silicon plates were immersed in a 3:1 piranha solution (98% H_2SO_4 and 30% H_2O_2) for 30 min at 25 °C. The plates were then thoroughly washed with ultrapure water that had undergone a three-stage purification process.

The implants were cut by using a BySprintFiber instrument with a FiberLaser 3 kW laser cavity and polished with 138 grit sandpaper (silicon carbide paper). Then, the implants were treated with piranha solution (15 min), followed by rinsing with distilled water.

2.3. Obtaining Multilayer Coatings

The substrate coatings were obtained using a DC-R dip coater (Nadetch Innovations, Navarra, Spain) with 0.01 M polyelectrolytes. The silicon wafers and implants were immersed in a 0.01 M PEI solution for 30 min to obtain a positive charge on the surface. Then, the substrates were immersed in a polyelectrolyte solution (PAA) with a negative charge to obtain multilayer films. The surface was then washed with a rinsing solution (pH of the rinsing solution = pH of polyelectrolyte) to remove weakly adsorbed polyelectrolyte molecules. The substrate was then similarly treated with a polycation solution (CHI) to return the surface charge to its original state. The adsorption (application) of polyanions and polycations was carried out sequentially for 1 min at 25 °C. After one cycle, a double layer of polyelectrolytes (bilayers) formed on the substrate surface. This process was repeated until n (PAA/CHI) bilayers were formed on the substrate surface.

CHX solutions were prepared at concentrations of 2, 0.05, 0.025, 0.0125, and 0.00625% from a commercial solution of 2% CHX digluconate. Coated substrates with n -bilayer PAA/CHI films were immersed in a 10 mL CHX solution for 24 h. The immersion process was carried out using the impregnation method. The general scheme for obtaining the antibacterial coatings based on PAA and CHI and further introduction of CHI into the multilayer coatings is presented in Figure 1.

All coating samples were stored in a refrigerator at 11–12 °C until further analysis of antibacterial activity and cytotoxicity weeks later.

2.4. Methods and Instrumental Characterization

2.4.1. Analysis of Surface Morphology and Topography.

The surface structure of the substrates with multilayer coatings and the impregnated antibacterial agent was characterized by scanning electron microscopy (SEM; Quanta 200i 3D, FEI Ltd., Hillsboro, OR, USA) and atomic force microscopy (AFM; Solver Spectrum, NT-MDT America Inc., Tempe, AZ, USA).

SEM of all specimens was performed at an accelerating voltage of 15 keV and a working distance of 12 mm according to the imaging options. The samples were secured with double-sided adhesive tape. All measurements were performed in high vacuum mode at 10^{-3} Pa. The maximum magnification was $\times 200$.

Energy-dispersive X-ray spectroscopy (EDX) was employed to determine the elemental composition of the samples by X-ray microanalysis via SEM. EDX was carried out at an acceleration voltage of 15 keV and a working distance of 15 mm.

AFM was utilized to obtain detailed information about the topography, roughness, and various physical properties of the surface. The measurements were performed in semicontact mode using an NSG01 probe, a standard silicon probe with a tip radius of 10 nm (the typical tip radius of curvature is 10 nm).

The thickness and growth of the dry film were determined by using an ELLIPS-1891-SAG spectral ellipsometer (CNT, Novosibirsk, Russia). Measurement of the spectral dependency of the ellipsometric angle was carried out at 250–1100 nm. The spectral resolution of the device was 2 nm; the recording time of one spectrum did not exceed 20 s, and the angle of incidence of the light beam on the sample was 70 °C. A four-zone measurement technique was employed, followed by averaging over all four zones.

2.5. Determination of Contact Angle

The sessile drop method was used with a DSA100 device (KRÜSS GmbH, Hamburg, Germany). The average drop diameter was 2–5 mm. The surface of the titanium implant was imaged in at least three areas due to the presence of irregularities.

2.6. CHX Release

The absorption spectrum of the CHX solution was measured using an EMS-11-UV spectrophotometer (EMCLAB Instruments, Duisburg,

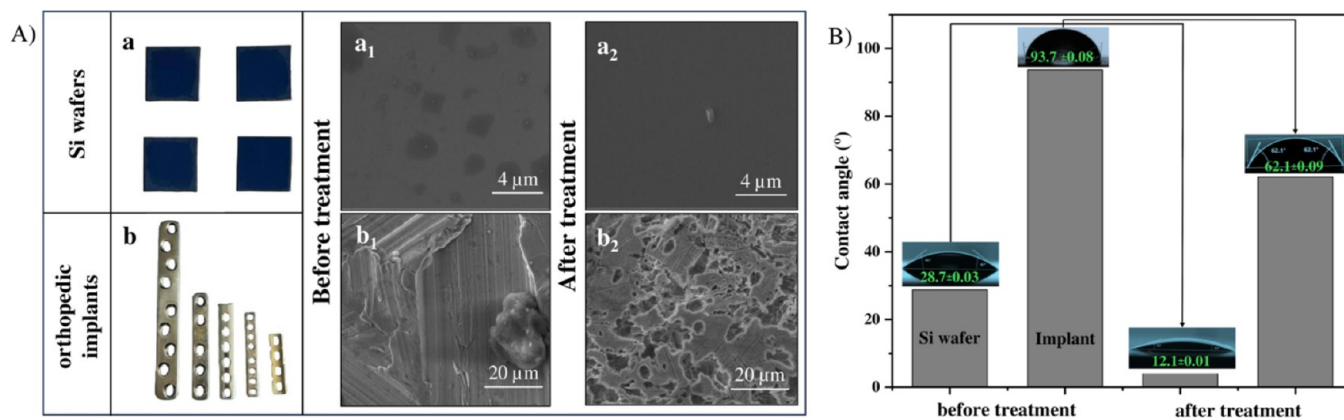


Figure 2. Surfaces of silicon wafers and implants before and after treatment (A) and changes in the contact angle of the substrate before and after treatment (B).

Germany). Different CHX concentrations ranging from 0.0125 to 2% (wavelength range of 170–400 nm) were used to generate a calibration curve. The absorption spectrum of the samples was recorded at 220 nm.

For the CHX release experiments, the implants were immersed in a 10 mL PBS solution at pH 7.4 and 37 °C for 48 h. Over this period, 2 mL of the release solution was removed every 2 h and replaced with 2 mL of fresh PBS. The optical density of CHX was continuously monitored at 220 nm via UV spectroscopy. CHX release was quantified using the calibration curve.

All studies were carried out at least in triplicate, and the arithmetic mean and standard deviation from the mean were calculated.

2.7. Assessment of Antibacterial Activity

The determination of antimicrobial activity was performed using the disk diffusion method according to the Performance Standards for Antimicrobial Disk Susceptibility Test, CLSI Vol. 30 No. 1, Jan 2010. The museum reference strains *S. epidermidis* ATCC 12228 and *S. aureus* ATCC 6538-P (Gram-positive strain, test culture from the American Type Culture Collection [ATCC, Manassas, VA, USA]) were employed as model bacteria. Mueller–Hinton agar (MHA) and a 0.9% NaCl solution (saline) were used for the samples. A detailed determination of the antibacterial activity by the disk diffusion method is described in ref 41. Three samples with coatings (with or without CHX) were placed on the surface of inoculated dishes. As a control, three plates without coatings were placed on similarly seeded Petri dishes. The cultures were incubated 37 ± 1 °C. The results were recorded by measuring the diameter of the culture growth inhibition after 6, 12, 24, 30, 36, and 48 h. To determine the ZI for one bacterial species, three identical samples were assessed. Based on the obtained results, the average values and standard deviations were calculated by using Excel. The results were analyzed according to the CLSI standard.

2.8. In Vitro Cytotoxicity Assays

Evaluation of sample cytotoxicity was performed in accordance with the requirements of national standard ISO 10993-5-2011 “Medical devices. Evaluation of the biological effects of medical devices, Part 5 (Republic of Kazakhstan)”. Human mononuclear cells (HMNCs) from peripheral whole blood were directly incubated with an extract from the coating, and cytotoxicity was measured using a colorimetric test based on the MTT method. To prepare an extract from the coating on the implant surface under aseptic conditions, the coated implant was placed in a presterilized Petri dish containing 10 mL of sterile medium for the cultivation of RPMI-1640 cells and incubated at 37 °C for 24 h. Extracts (1/2, 1/4, etc.) were obtained by serial dilution of 100% extract in the culture medium. After HMNCs were reseeded onto a 96-well plate at a rate of 20,000 cells per well, the extracts were added. After incubation, the medium containing the extract was removed from the wells; the cells were washed once with 200 μL of 1× PBS, and 100 μL of culture medium containing 10 μL

of MTT was added to each well. The plates were incubated at 37 °C for 4 h. Then, the incubation medium with dye was carefully removed, and 100 μL of DMSO was added. Optical density measurements were performed using a Tecan Sunrise spectrophotometer (Tecan Group Ltd., Männedorf, Switzerland) at 540 nm (reference, 620 nm).

Cell viability (%) was calculated for each replicate of each dilution using the formula:

$$\text{viability, \%} = \frac{Y_i}{\bar{Y}_{\text{NC}}} \times 100\%$$

where Y_i is the measured optical density (OD) for each group, and \bar{Y}_{NC} is the arithmetic mean of the OD for the negative control.

The standard deviation (StD) was calculated using the following formula:

$$\text{StD} = \sqrt{\sum_{i=1}^n (Y_i - \bar{Y})^2 / (n - 1)}$$

where n is the number of objects in the group, and \bar{Y} is the arithmetic mean value of the OD.

All studies were carried out in triplicate, and the arithmetic mean and standard deviation from the mean were calculated.

3. RESULTS AND DISCUSSION

3.1. Characterization of Silicon and Titanium Substrates

To ensure biocompatibility and prevent bacterial biofilm formation on the surfaces of implants, we modified the surface of orthopedic implants by introducing CHX into a PEM coating. One of the most important aspects in the development of such coatings is the modification of the implant surface. This process aims to create a developed surface that can interact with chemical reagents and base material. Particular attention should be given to surface modification methods that control the charge of the biomaterial's surface, such as changing the morphology and contact angle of the surface by activation. Since the substrate surface was initially undeveloped, the implants and silicon wafers were etched with piranha solution, which consists of concentrated H₂SO₄ and HCl, and SEM was employed to analyze the surface, structure, and morphology of the substrates before and after treatment (Figure 2A).

The results indicated that a non-uniform oxide layer formed on the surface of the silicon wafers and that adsorbed particles were present. Oxide films can form on silicon wafers during storage, making the adsorption of water-soluble polymers difficult due to their low binding energy. As expected, treatment with piranha solution completely removed impur-

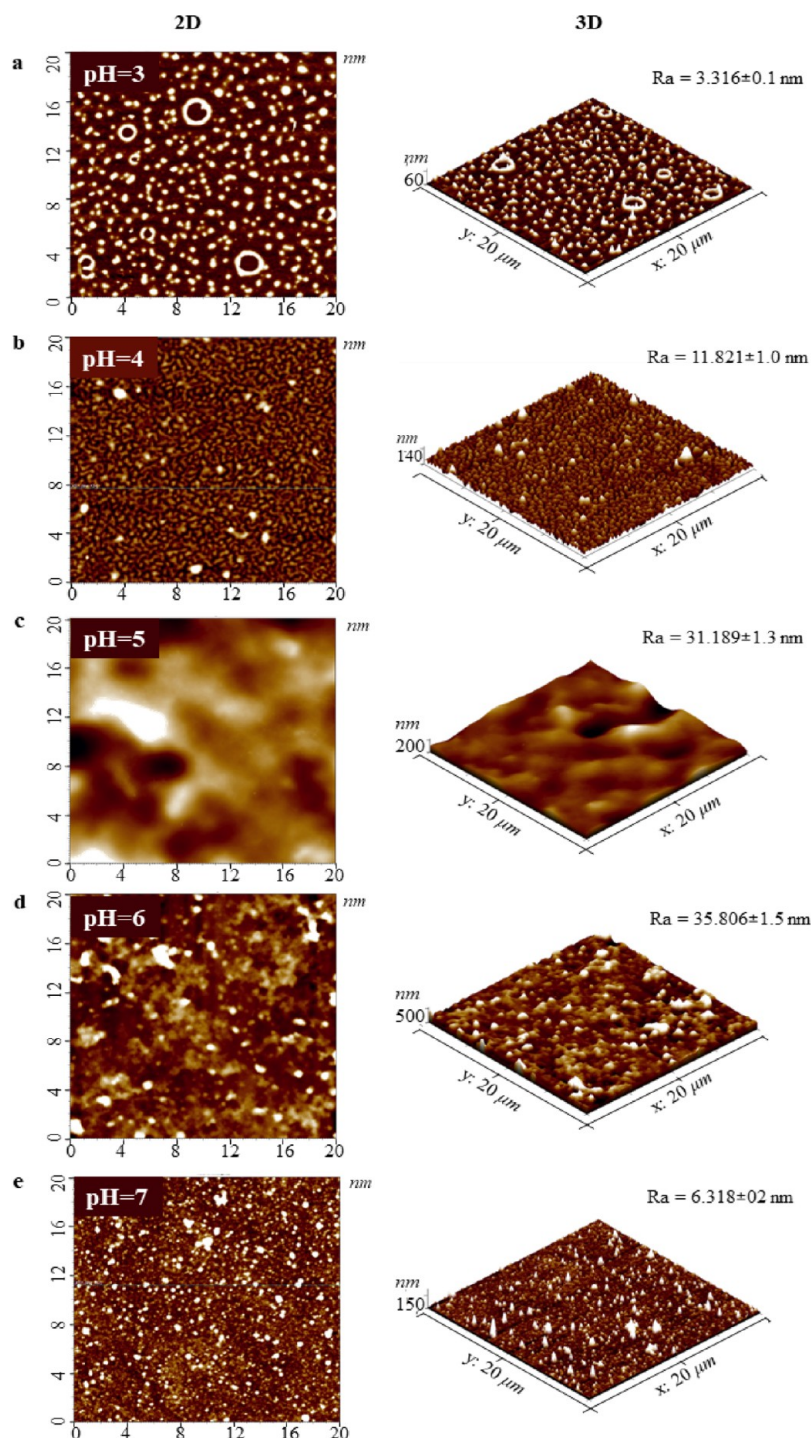


Figure 3. Two-dimensional and 3D AFM images of (PAA/CHI)_{14.5} thermally cross-linked LbL films obtained at pH 3–7 (a–e). Roughness values were recorded from images with a $20 \times 20 \mu\text{m}^2$ scan size.

ities from the surfaces of the silicon wafers. In the case of the implants, their surface was polished before etching, which, according to Nazarov et al.,⁵⁷ ensures uniform and consistent etching. The results clearly showed the formation of microcracks on the implant surface after etching, which contributed to better adhesion of the polyelectrolytes. These results were explained by H_2SO_4 in piranha solution dissolving the oxide film, while H_2O_2 provided atomic oxygen, which oxidized organic and inorganic impurities on the sample surface. The obtained results were in good agreement with the work by

Nazarov et al.,⁵⁷ who also noted the formation of microcracks on the implant surface as a result of prolonged treatment (several hours or more), with kinetic control. In a similar study conducted by Mukaddam et al.,⁵⁸ an increase in the average surface roughness was noted after etching, which reduced the adhesion of bacteria and prevented biofilm formation.

The increased hydrophilicity of the biomaterial surface is known to improve the healing process.^{59,60} To monitor changes in the physicochemical characteristics of the surface, the sessile drop method was used to measure changes in the

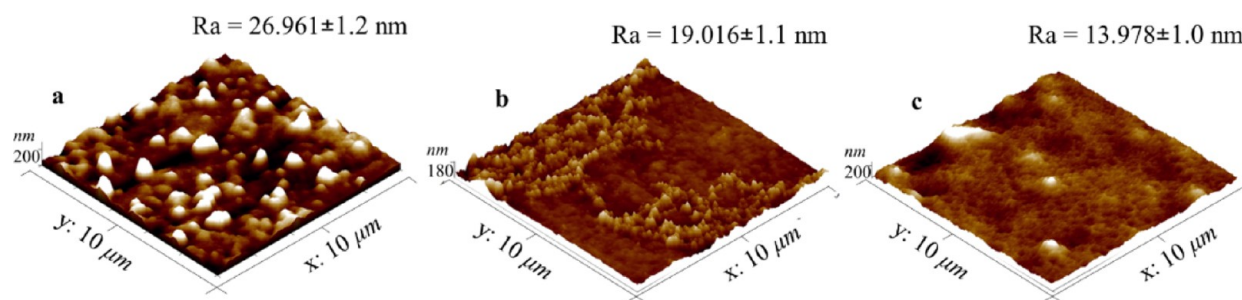


Figure 4. AFM images of (PAA/CHI)_{14.5} films before (without (a) and with (b) thermal cross-linking) and after (c) CHX (0.025%) loading. Roughness values were recorded from images with a $10 \times 10 \mu\text{m}^2$ scan size.

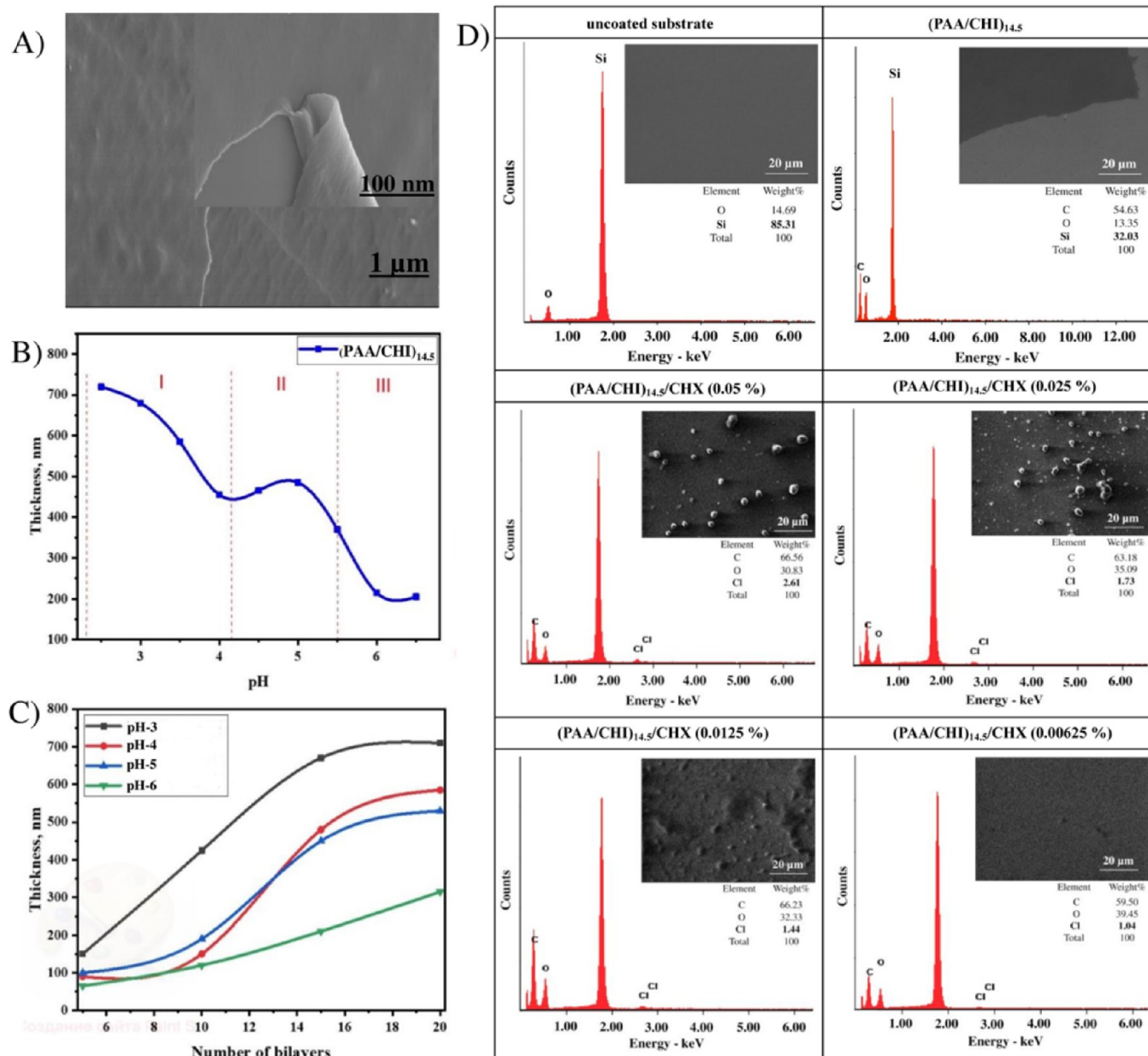


Figure 5. SEM images of coating (A), dependence of dry film (PAA/CHI)_{14.5} thickness on pH assembly (B), film growth at different pH assemblies (C), and SEM/EDX spectra of uncoated and coated substrates (D).

surface contact angle before and after treatment (Figure 2B). The contact angle after treatment decreased compared to that of the original material. That is, the chemical treatment made it

possible to further increase the hydrophilicity of the surface. For example, the contact angle of the surface of titanium implants before etching was $93.7 \pm 0.08^\circ$, while it decreased to

$62.1 \pm 0.09^\circ$ after treatment. In the case of the silicon wafers, a more than 2-fold decrease in the surface contact angle was observed, resulting in pronounced hydrophilicity. Thus, the changes in the contact angle confirmed the changes in the physicochemical characteristics of the surface after treatment, which indicated the successful modification of the surface.

3.2. Characterization of Nanocoatings

3.2.1. AFM Analysis of Nanocoatings. A PAA/CHI-based coating was selected as a reservoir for the delivery of CHX. The use of weak polyelectrolytes made it possible to control the roughness and morphology of the coatings by changing the polyelectrolyte pH. The ionizable groups in the multilayer polyelectrolytes responded to pH fluctuations, effectively regulating the drug delivery process.

Two-dimensional and 3D images of the surface of the LbL coating (PAA/CHI)_{14,5} were obtained via AFM, revealing changes in the average roughness as a function of the change in pH of the LbL coating assembly, ranging from pH 3 to 7 (Figure 3).

The average roughness increased from 3.316 ± 0.1 to 35.806 ± 1.5 nm. However, a strong decrease in surface roughness could be observed at the transition from pH 6 to 7, which was due to the molecules in this range behaving as strong polyelectrolytes, leading to the formation of flat films.⁶¹ In general, smoother films were obtained at pH 3 and 4, with corresponding roughness values of 3.316 ± 0.1 and 11.821 ± 1.0 nm, respectively (Figure 3a,b). This was due to the extended conformation of the polycation in this region, which promoted the compact packing of chains during film formation. However, the rougher surfaces observed at pH 5 and 6 (Figure 3c,d) were attributed to the relatively weak interaction between CHI and PAA, which led to the formation of various loops and tails in the multilayer structures and contributed to increased surface roughness. The formation of a rough surface, depending on the assembly process conditions, was mainly due to the structure of PAA rather than that of CHI. As previously reported,⁶² PAA is more susceptible to pH changes in the medium than CHI and has a spiral and looplike structure. The properties of polyelectrolytes, such as chain length and charge density, are strongly dependent on pH.^{61,63} Coatings obtained at pH 3 and 4 exhibited approximately the same height difference across the surface, which corresponded to low roughness. In addition, a granular surface structure was observed, especially at pH 7 (Figure 3e), although its character was not as uniform as at lower pH values. The noticeable difference in the roughness of the coatings obtained at pH 5 (Figure 3c) compared with other samples was attributed to the complexation of polyelectrolytes.

The efficient integration of CHX into (PAA/CHI)_{14,5} coatings is of great interest for surface research and modification. In this context, an analysis of the morphological changes on the surface before and after CHX introduction was carried out. CHX was integrated into the coating composition at pH 6 because of its rough, developed surface at this pH. Figure 4 presents the AFM results of a multilayer coating before and after exposure to CHX and AFM images of the coating before and after thermal cross-linking. A comparison of the surface morphology of the multilayer structures before and after thermal cross-linking reflected a smoothing of the surfaces with a parallel decrease in roughness from 26.961 ± 1.2 nm (Figure 4a) to 19.016 ± 1.1 nm (Figure 4b). This was

attributed to the release of a water molecule from the coating after thermal cross-linking.

When treating the multilayer coated substrate with a CHX solution, low-molecular-weight compounds were likely adsorbed to the top and bottom structures of the film. This likely led to partial filling of the voids formed during the layering of polyelectrolytes. As a result, the surface roughness was observed to decrease from 19.016 ± 1.1 nm for (PAA/CHI)_{14,5} (Figure 4b) to 13.978 ± 1.0 nm for (PAA/CHI)_{14,5}/CHX (Figure 4c). In addition, although coatings without CHX had a maximum peak at 180 nm (Figure 4b), this value increased to 200 nm after CHX introduction (Figure 4c), while the average roughness decreased. This was observed as a decrease in the abundance of sharp drops in the peaks. A similar dependence was reported by Cagli et al.⁶⁴ after the introduction of an antibiotic.

3.2.2. Film Growth and SEM/EDX Analysis. As shown in the SEM images (Figure 5A), the coatings exhibited a layered structure, stacked one after the other, confirming the formation of a thin film on the surface. Since the coatings were developed based on weak polyelectrolytes, studying their thickness and growth was interesting. Control over the thickness and molecular architecture of such films can be achieved by optimizing the pH of the solution during the deposition of weak polyelectrolytes.⁶³ As can be seen from Figure 5B, the thickness of the films varied with the pH in three regions. Thicker coatings were formed at low pH values, while the thinnest films were observed in region III, which was likely due to differences in the degree of ionization of the polyelectrolytes and their conformation at different pH values. The growth of the dry PAA/CHI film as a function of the number of bilayers was also examined (Figure 5C). At high pH values, a linear change in thickness was observed, while the growth was exponential at low pH values, which was likely due to the diffusion of polymer chains through the multilayer structures.

SEM/EDX (Figure 5D) was utilized to analyze the elemental composition of the coated and uncoated substrates. Uncoated silicon wafers consisted of the elements silicon (Si) and oxygen (O). After a coating consisting of PAA and CHI was obtained, the elemental composition of the surface changed. As expected, the altered surface contained elements such as carbon (C) and oxygen (O), and no chlorine (Cl) peaks were observed.

The composition of coatings containing CHX at different concentrations for impregnation revealed the presence of Cl atoms, which are one of the main indicators of the presence of CHX in the samples. In general, Cl atoms were found in the elemental composition of all coatings containing CHX. With a decrease in the CHX concentration used for impregnation, the mass fraction of Cl in the coating also decreased. For example, the mass fraction of Cl in a coating impregnated with 0.05% CHX was 2.61%, while it was 1.04% when a low CHX concentration was used (0.00625%), demonstrating a 2.5-fold reduction.

3.3. Antibacterial Activity Results

3.3.1. Study of the Antibacterial Activity of PAA/CHI/CHX Nanocoatings Obtained at Different pH Assemblies. PEMs assembled by electrostatic interaction of polyelectrolytes, which combine the characteristic properties of high- and low-molecular-weight compounds, can be potential reservoirs for the delivery of antibacterial agents. Herein, CHX bigluconate, a low-molecular-weight antiseptic,

was used as the antibacterial agent because it is a gold standard antiseptic that is active against Gram-positive/negative bacteria and, unlike antibiotics, does not show resistance after long-term use.³⁷

Loading and release of the antibacterial agent depend on various factors, such as the conditions under which the reservoir is formed and the nature of the reservoir itself.⁶⁴ Herein, the effect of the assembly pH on the antibacterial activity of the (PAA/CHI)_{14.5} multilayer coating containing CHX was investigated. CHX was integrated into the coating structure, and the pH of the assembly was varied from pH 3 to 7. The top layer of the film was coated with PAA, and CHX was assumed to be incorporated into the PEM structures through electrostatic interaction. Two pK_a values are known for CHX, 10.3 and 2.2, and CHX behaves as a bicationic (+2) compound at pH 4–8. In general, low-molecular-weight CHX contains four imine groups (C=NH) and amine groups (C–NH) in its structure.³⁹

The obtained coatings were tested for activity against Gram-positive *S. aureus* ATCC 6538-P (Figure 6), considering that staphylococci are the predominant bacterial agents predisposed to biofilm formation and subsequent development of implant-associated infections, accounting for 50–60% of the total

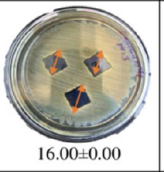
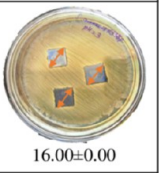

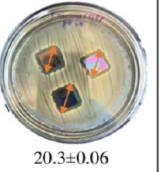

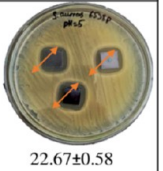

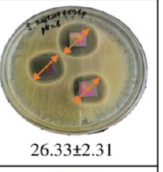
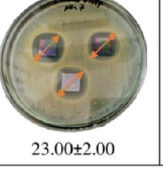
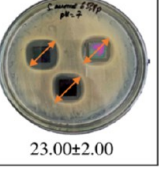
Si substrates	Zone of inhibition, mm ± StD	
	<i>Staphylococcus aureus</i> ATCC 6538-P	
	24 h	72 h
pH=3	 16.00±0.00	 16.00±0.00
pH=4	 20.3±0.06	 20.3±0.06
pH=5	 22.67±0.58	 22.67±0.58
pH=6	 26.33±2.31	 26.33±2.31
pH=7	 23.00±2.00	 23.00±2.00

Figure 6. Antibacterial activity of LbL coatings (PAA/CHI)_{14.5}/CHX (0.05%) obtained at different pH assemblies against *S. aureus* ATCC 6538-P after exposure for 24 and 72 h.

number of cases. The antibacterial potential of the coatings obtained at different pH assemblies on the surface of silicon wafers was studied using the disk diffusion method. The results obtained after incubation for 24 and 72 h revealed that the coating obtained at pH 6 exhibited higher antibacterial activity than those obtained at other pH assemblies. This was attributed to the formation of a rougher structure, which enabled increased loading of CHX compared to other assembly conditions.

Notably, in all cases, the antibacterial activity of the coatings was maintained with increased suspension density for 72 h, indicating the stability of the effect. The reduced activity at low pH was due to the weak ionization of PAA, resulting in only a small amount of positively charged CHX binding to the material. In addition, a smoother surface limited the penetration of CHX into the interlayer. Moreover, aqueous CHX solutions are the most stable at pH 5–8, while a gradual deterioration is observed under more acidic conditions.³⁹

The effect of LbL assembly pH was also investigated by Shiratori and Rubner,⁶³ who noted that the HA/CHI film assembled at pH 7.2 exhibited superior loading capacity and longer release of Rose Bengal compared to the film assembled at pH 4.5. This effect was associated with the higher roughness and lower hydrophilicity of the film obtained at pH 7.2 than at pH 4.5. The work by Cagli et al.⁶⁴ also highlighted the role of film surface topology in drug release (ciprofloxacin) and antibacterial properties. Thick and loose PAA/CHI multilayer films released more ciprofloxacin and thus exhibited increased antibacterial activity compared with thin and more intense tannic acid/CHI films.

The study findings confirmed the importance of the influence of the pH on the characteristics of multilayer coatings and their bioactivity. That is, tuning even one parameter, such as the pH, provided a greater understanding of the formation process of PAA/CHI films and their use as a matrix for the storage and delivery of CHX.

In addition, the antibacterial effect of the coating was investigated before and after CHX inclusion (Figure 7). PEM coatings represent an important tool for the surface functionalization of biomaterials, wherein the drug substance introduced by impregnation is integrated into the multilayer

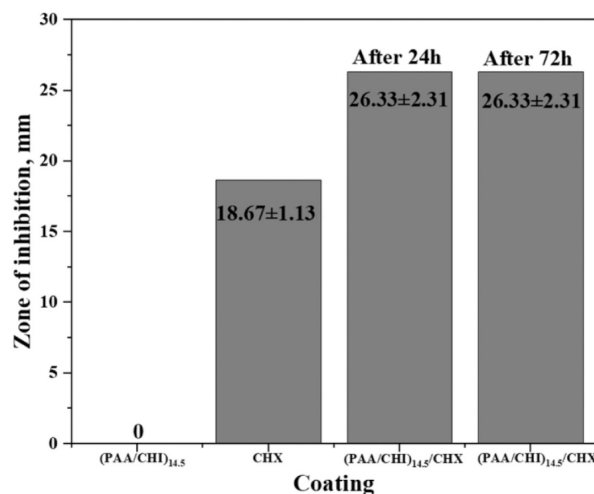


Figure 7. Antibacterial activity of coatings with different compositions against *S. aureus* ATCC 6538-P.

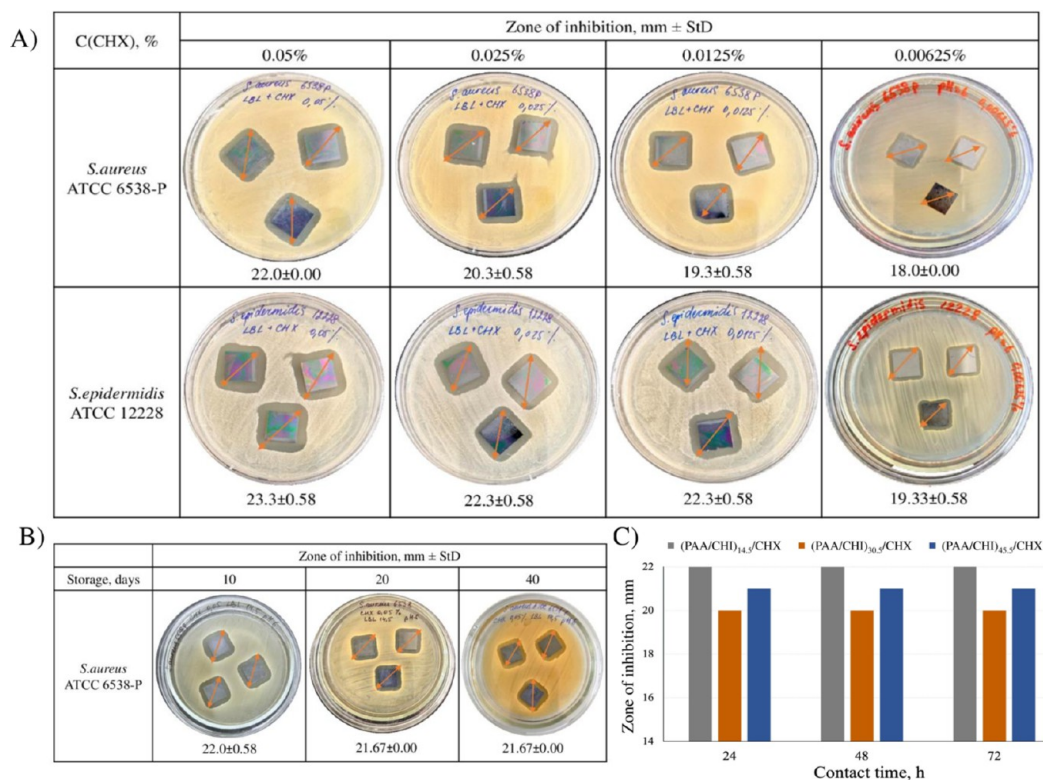


Figure 8. Antibacterial activity of coatings at different CHX concentrations against *S. aureus* ATCC 6538-P and *S. epidermidis* ATCC 12228 after exposure for 24 h (A), activity of aged coating during storage (B), and evaluation effect of the number of bilayers on activity (C).

structure, making this method applicable to a wide range of drugs.^{65–69}

The obtained results demonstrated that the (PAA/CHI)_{14.5}/CHX coating exhibited higher antibacterial activity (26.33 ± 2.31), while simple impregnation of the substrate with CHX without the use of PEM structures exhibited lower activity (18.67 ± 1.13). Interestingly, the sample consisting solely of polyelectrolytes (PAA/CHI) did not provide protection against bacterial colonization.

The appearance of the ZI around the sample impregnated with pure CHX was attributed to the impregnation of CHX onto the solid substrate, which acquired a negative charge after treatment with piranha solution. This resulted in chemical bonding between the modified surface of the solid substrate and CHX. Despite the antibacterial effect observed in the sample coated with CHX alone, ZI completely disappeared after exposure of the bacteria for 24 h. At that time, PEM coatings with embedded CHX exhibited activity even after 3 days. Moreover, the use of PEM structures increased the bacterial activity and prolonged the duration of action due to the prolonged release of CHX.⁴⁰ A similar study conducted by de Villiers et al.⁷⁰ confirmed the importance of PEM coatings as a drug delivery system.

3.3.2. Effect of CHX Concentration on the Activity and Assessment of Coating Aging. The antimicrobial effect of CHX depends on its concentration. Herein, (PAA/CHI)_{14.5} multilayer coatings were immersed in different CHX concentrations (0.05–0.00625%), which were chosen to systematically study the change in coating activity when the CHX concentration was halved from the previous concentration. This approach made it possible to identify patterns and changes with each subsequent decrease in CHX concentration. Then, antibacterial activity was assessed against two model

bacteria, *S. aureus* and *S. epidermidis*. The results were measured after the bacteria were exposed to the coatings for 24 h. In general, greater activity was observed against *S. epidermidis* ATCC 12228 than *S. aureus* ATCC 6538-P (Figure 8A).

As shown in Figure 8A, ZI demonstrated a pronounced increase with increased CHX concentration used for impregnation from 0.00625 to 0.05%. However, it is important to note that the ZI around the coating impregnated with a low CHX concentration (0.00625%) did not substantially differ from that obtained for the coating impregnated with a high CHX concentration (0.05%). For example, for *S. epidermidis* ATCC 12228, the ZI around the sample coated with (PAA/CHI)_{14.5}/CHX (0.05%) was 23.3 ± 0.58 mm, while it was 19.33 ± 0.58 mm for (PAA/CHI)_{14.5}/CHX (0.00625%), which was 4 mm less. The increase in the ZI depending on the CHX concentration was attributed to an increase in the number of active CHX molecules on the bacterial surface when the concentration changed from 0.00625 to 0.05%. These results were confirmed by EDX (Figure 5D). The mechanism of action of CHX is the dissociation of its salts, which leads to the release of cationic ions. These ions are adsorbed onto the cell membrane, disrupting its integrity and causing leakage of intracellular contents. Penetrating into the cell, the ions interact with cytoplasmic components, inhibiting protein synthesis and inducing osmotic stress, which leads to the death of bacteria.³⁶

The study of aged coating activity against *S. aureus* ATCC 6538-P was carried out after storage for 10, 20, and 40 days (Figure 8B), revealing that the activity of the coating was practically unchanged during this time interval. Specifically, coatings stored for 10 and 40 days exhibited ZIs of 22.0 ± 0.00 and 20.67 ± 0.58 mm, respectively. The results indicated the




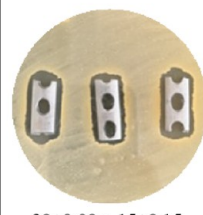




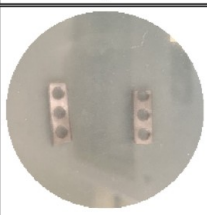



Contact time (h.)	Zone of inhibition, mm \pm StD			
	6	24	48	72
Sample (a)	 0	 30 \pm 0.00 x 15 \pm 0.15	 30 \pm 0.00 x 15 \pm 0.15	 30 \pm 0.00 x 15 \pm 0.15
Sample (b)	 0	 28 \pm 0.00 x 15 \pm 0.00	 28 \pm 0.00 x 15 \pm 0.00	 28 \pm 0.00 x 15 \pm 0.00
Sample (c)	 0	 27.5 \pm 0.00 x 15 \pm 0.00	 27.5 \pm 0.00 x 15 \pm 0.00	 28 \pm 0.00 x 15 \pm 0.00

Figure 9. Antibacterial activity of coating on implants intended for the lower leg (sample a), collarbone (sample b), and tibia fibula (sample c) after a certain time (6 to 72 h) of contact with *S. aureus* ATCC 6538-P.

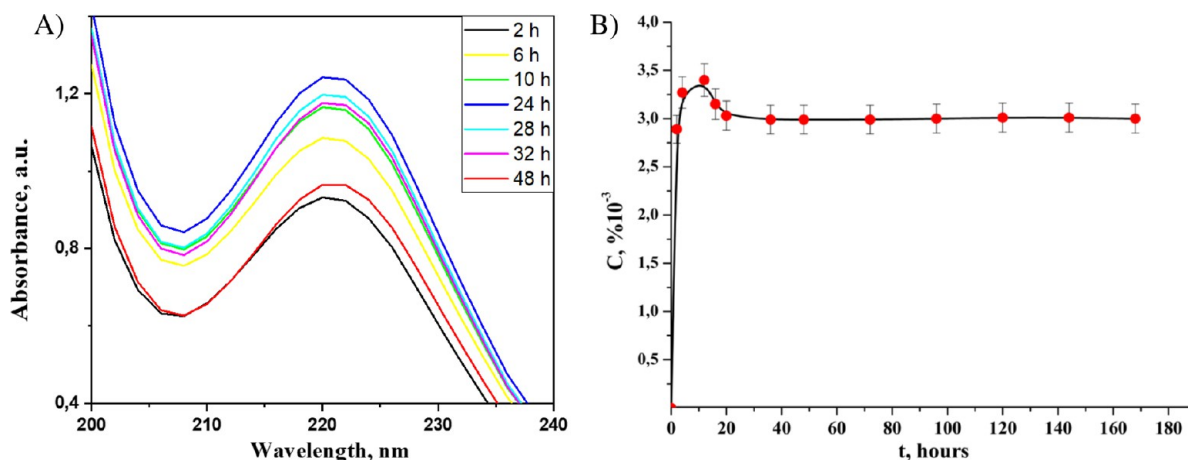


Figure 10. Absorption spectra of the released CHX solution at different time intervals (A) and release of CHX at different times (B).

stability of the coating during storage and allowed us to conclude that CHX was not washed out of the coating during storage.

In addition, CHX was incorporated into coatings consisting of 14.5, 30.5, and 45.5 bilayers. Analysis of the results demonstrated that increasing the number of bilayers did not lead to a significant increase in the antibacterial activity of the coatings (Figure 8C). The zone of inhibition (ZI) remained unchanged during the studied incubation period (24–72 h), which was likely due to CHX being more easily diffused and released from the 14.5 bilayer coating than from the 45.5 bilayer coating. It is also possible that CHX, located in the inner layers of thicker coatings, was less accessible to interact

with bacteria on the surface. In this way, coating structures could be optimized to ensure maximum antibacterial activity.

3.3.3. Evaluation of Antibacterial Activity of Coatings on Implants Depending on Contact Time. The manifestation of the ZI depends not only on the concentration of the drug but also on the time of exposure to bacteria.³⁶ For this purpose, coated implants were exposed to bacteria and incubated for various times (6 to 72 h). The ZI diameter around the implants was measured after a certain duration of contact with bacteria. Figure 9 presents the ZIs around various implants intended for the tibia (sample a), clavicle (sample b), and tibia fibula (sample c).

As can be seen in Figure 9, despite the rather low density of the suspension, no ZI formed in the first 6 h. However, ZI

appeared during subsequent exposure to the implants. The ZI recorded after 24 h remained unchanged until the end of the measurement period (72 h). Thus, the coating remained active due to active growth of the test strain. The obtained results demonstrated the potential antibacterial activity of nanofilms based on CHI/PAA/CHX deposited on the surfaces of real titanium implants.

3.4. Drug Release from Multilayer Coatings

Figure 10 presents the dynamics of CHX release from the (PAA/CHI)_{14.5}/CHX (0.025%) coating on the implant surface. For calibration, solutions of pure CHX digluconate were used from 0.003 to 0.02%. The absorption spectra of the standard solutions were measured from 170 to 400 nm, while the absorption spectra of the eluted solution obtained at each time interval were recorded at 220 nm (Figure 10A).

The graph presented in Figure 10B shows the continuous release of drug from the (PAA/CHI)_{14.5}/CHX coatings over a period of 168 h. In the first 16 h, a sharp release of chlorhexidine into the solution is observed, which can be explained by the diffusion of unbound CHX from the top layer of the coating.⁷¹ This effect is likely enhanced by weak and nonspecific interactions of CHX with the coating, such as hydrogen and electrostatic bonds.⁷² Subsequently, over longer time intervals, a monotonous release of CHX from PEMs is observed due to the dynamic expansion and swelling of the polymer layer, which requires a certain time to displace CHX.

The study recorded a sustained release of the drug over 168 h, indicating its prolonged action. It is worth noting that a certain part of the antibacterial drug remains in the composition of the coatings, supporting the further release of CHX, since after 7 days, its concentration did not reach zero. Thus, drug release, characterized by slow diffusion, will provide long-lasting pathogen suppression and long-term protection of the biomaterial.

3.5. In Vitro Cytotoxicity Study

Experiments to evaluate the biocompatibility of the coated substrate were performed on HMNCs and quantified using the MTT assay. The cytotoxicity of the samples was assessed in accordance with the requirements of the state standard ISO 10993-5-2011. Figure 11 presents the cell viability results at various concentrations of the extract obtained from coatings with different compositions on titanium implants. The duration of exposure of HMNCs to the extracts was 48 h under CO₂ conditions in an incubator. The various extract concentrations, 50, 25, 12.5, 6.25, 3.125, and 1.5625%, corresponded to 1/2, 1/4, 1/8, 1/16, 1/32, and 1/64 dilutions of the original extract, respectively.

As shown in Figure 11, a decrease in the extract concentration led to an increase in the number of living cells. As expected, the viability of HMNCs in all dilutions of the extract obtained from the coating without CHX was higher than that of HMNCs in the extracts containing CHX. The high viability of HMNCs in extracts obtained from the coating without CHX was due to the low concentration of polymers (PAA and CHI) and the biocompatibility of the polyelectrolytes that formed the basis of the LbL coating. Thus, the viability of HMNCs > 81.33% in the tested dilution range of 1/64–1/2 of the original extract.

Cell viability also depended on the CHX concentration introduced into the coating composition. As expected, the cell viability was higher at a low CHX concentration in the coating (0.0125%), while the (PAA/CHI)_{14.5}/CHX (0.05%) coating

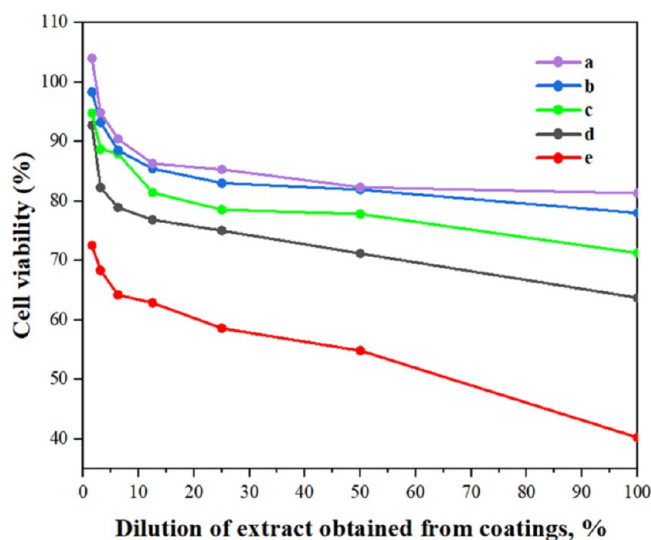


Figure 11. Cytotoxicity of extracts from implants with coatings of different compositions: (a) (PAA/CHI)_{14.5}, (b) (PAA/CHI)_{14.5}/CHX (0.0125%), (c) (PAA/CHI)_{14.5}/CHX (0.025%), (d) (PAA/CHI)_{14.5}/CHX (0.05%), and (e) CHX (0.05%).

showed mild cytotoxicity. This was attributed to the (PAA/CHI)_{14.5}/CHX (0.05%) coating having a higher drug content than the (PAA/CHI)_{14.5}/CHX (0.025%) and (PAA/CHI)_{14.5}/CHX (0.0125%) coatings. Notably, the cell viability observed for the (PAA/CHI)_{14.5}/CHX (0.0125%) coating did not substantially differ from that in the absence of CHX. This was due to the low CHX concentration present in this coating and its controlled release. Also noteworthy were the results obtained with implants coated with pure 0.05% CHX, where moderate cytotoxicity was observed. Cell viability ranged from $40.27 \pm 5.29\%$ to $72.57 \pm 6.18\%$ depending on the dilution of the original extract. This was due to the sudden release of CHX when extracts were obtained from implants coated with pure CHX solution. Thus, the results demonstrated the importance of PEMs in the formation of coatings with low cytotoxicity due to the controlled release of CHX. The obtained results aligned with those of a previous study⁷³ reporting the high cytocompatibility of a coating on a catheter with CHX encapsulated in micelles. The high biocompatibility of the developed coating supports its potential for further use in biomedicine.

4. CONCLUSIONS

The study demonstrated that antibacterial coatings based on PAA/CHI/CHX can be effectively used in orthopedic implants. The optimal pH for the introduction of CHX into the coating composition was determined to be 6, which made it possible to individualize the coating surface and its architectural features. The surface roughness and topography changed after CHX introduction, providing different zones of bacterial inhibition. Antibacterial activity depended on the CHX concentration and the time of contact between the coating and bacteria.

The coatings maintained antibacterial activity during storage and demonstrated continuous CHX release for 48 h. Cell viability was higher when cells were exposed to extracts of coatings without CHX, whereas exposure of cells to extracts of coatings with CHX induced moderate cytotoxicity. A

limitation of the study is the lack of data about the osseointegration of such coatings.

Thus, the obtained coatings demonstrated antibacterial properties and cytocompatibility, making them promising for use in biomedical applications.

AUTHOR INFORMATION

Corresponding Author

Balzhan Savdenbekova – Faculty of Chemistry and Chemical Technology, Al-Farabi Kazakh National University, Almaty 050040, Kazakhstan; Center of Physical–Chemical Methods of Research and Analysis, Almaty 050012, Kazakhstan; orcid.org/0000-0001-8812-5809; Email: balzhan.savdenbekova@gmail.com

Authors

Ayazhan Seidulayeva – Faculty of Chemistry and Chemical Technology, Al-Farabi Kazakh National University, Almaty 050040, Kazakhstan; Center of Physical–Chemical Methods of Research and Analysis, Almaty 050012, Kazakhstan

Aruzhan Sailau – Faculty of Chemistry and Chemical Technology, Al-Farabi Kazakh National University, Almaty 050040, Kazakhstan; Center of Physical–Chemical Methods of Research and Analysis, Almaty 050012, Kazakhstan

Zhanar Bekissanova – Faculty of Chemistry and Chemical Technology, Al-Farabi Kazakh National University, Almaty 050040, Kazakhstan; Center of Physical–Chemical Methods of Research and Analysis, Almaty 050012, Kazakhstan

Dilafruz Rakhmatullayeva – Faculty of Chemistry and Chemical Technology, Al-Farabi Kazakh National University, Almaty 050040, Kazakhstan; Center of Physical–Chemical Methods of Research and Analysis, Almaty 050012, Kazakhstan

Ardak Jumagaziyeva – Scientific Center for Anti-Infectious Drugs, Almaty 050060, Kazakhstan

Complete contact information is available at:

<https://pubs.acs.org/10.1021/acspolymersau.4c00049>

Author Contributions

CRedit: **Balzhan Savdenbekova** conceptualization, methodology, writing-original draft; **Ayazhan Seidulayeva** investigation, methodology, validation; **Aruzhan Sailau** investigation, methodology, validation; **Zhanar Bekissanova** supervision, writing-review & editing; **Dilafruz Rakhmatullayeva** formal analysis, visualization; **Ardak Jumagaziyeva** investigation, methodology, resources.

Funding

This work was supported by the Science Committee of the Ministry of Science and Higher Education of the Republic of Kazakhstan (grant no. IRN AP19577150, “Study of prolongation properties and cytotoxicity of antibacterial films for implantable products based on natural polysaccharides containing chlorhexidine and silver nanoparticles”).

Notes

The authors declare no competing financial interest.

ABBREVIATIONS

LbL, layer by layer; CHI, chitosan; PAA, poly(acrylic acid); CHX, chlorhexidine; PEI, poly(ethylenimine); HMNC, human mononuclear cells; ZI, zone of inhibition

REFERENCES

- (1) Tejwani, N. C.; Immerman, I. Myths and Legends in Orthopaedic Practice: Are We All Guilty? *Clin Orthop Relat Res* **2008**, *466* (11), 2861–2872.
- (2) Spriano, S.; Yamaguchi, S.; Bairo, F.; Ferraris, S. A Critical Review of Multifunctional Titanium Surfaces: New Frontiers for Improving Osseointegration and Host Response, Avoiding Bacteria Contamination. *Acta Biomater* **2018**, *79*, 1–22.
- (3) Chug, M. K.; Brisbois, E. J. Recent Developments in Multifunctional Antimicrobial Surfaces and Applications toward Advanced Nitric Oxide-Based Biomaterials. *ACS Materials Au* **2022**, *2* (5), 525–551.
- (4) Udduttula, A.; Jakubovics, N.; Khan, I.; Pontiroli, L.; Rankin, K. S.; Gentile, P.; Ferreira, A. M. Layer-by-Layer Coatings of Collagen–Hyaluronic Acid Loaded with an Antibacterial Manuka Honey Bioactive Compound to Fight Metallic Implant Infections. *ACS Appl. Mater. Interfaces* **2023**, *15* (50), 58119–58135.
- (5) Wang, M.; Tang, T. Surface Treatment Strategies to Combat Implant-Related Infection from the Beginning. *J. Orthop Translat* **2019**, *17*, 42–54.
- (6) Arciola, C. R.; Campoccia, D.; Montanaro, L. Implant Infections: Adhesion, Biofilm Formation and Immune Evasion. *Nat. Rev. Microbiol* **2018**, *16* (7), 397–409.
- (7) Oliveira, W. F.; Silva, P. M. S.; Silva, R. C. S.; Silva, G. M. M.; Machado, G.; Coelho, L. C. B. B.; Correia, M. T. S. Staphylococcus Aureus and Staphylococcus Epidermidis Infections on Implants. *Journal of Hospital Infection* **2018**, *98* (2), 111–117.
- (8) Chessa, D.; Ganau, G.; Spiga, L.; Bulla, A.; Mazzarello, V.; Campus, G. V.; Rubino, S. Staphylococcus Aureus and Staphylococcus Epidermidis Virulence Strains as Causative Agents of Persistent Infections in Breast Implants. *PLoS One* **2016**, *11* (1), No. e0146668.
- (9) Decher, G.; Hong, J. D.; Schmitt, J. Buildup of Ultrathin Multilayer Films by a Self-Assembly Process: III. Consecutively Alternating Adsorption of Anionic and Cationic Polyelectrolytes on Charged Surfaces. *Thin Solid Films* **1992**, *210–211*, 831–835.
- (10) Ariga, K.; Hill, J. P.; Ji, Q. Layer-by-Layer Assembly as a Versatile Bottom-up Nanofabrication Technique for Exploratory Research and Realistic Application. *Phys. Chem. Chem. Phys.* **2007**, *9* (19), 2319.
- (11) Zhao, S.; Caruso, F.; Dähne, L.; Decher, G.; De Geest, B. G.; Fan, J.; Feliu, N.; Gogotsi, Y.; Hammond, P. T.; Hersam, M. C.; Khademhosseini, A.; Kotov, N.; Loporatti, S.; Li, Y.; Lisdat, F.; Liz-Marzán, L. M.; Moya, S.; Mulvaney, P.; Rogach, A. L.; Roy, S.; Shchukin, D. G.; Skirtach, A. G.; Stevens, M. M.; Sukhorukov, G. B.; Weiss, P. S.; Yue, Z.; Zhu, D.; Parak, W. J. The Future of Layer-by-Layer Assembly: A Tribute to ACS Nano Associate Editor Helmuth Möhwald. *ACS Nano* **2019**, *13* (6), 6151–6169.
- (12) Ariga, K.; Ahn, E.; Park, M.; Kim, B. Layer-by-Layer Assembly: Recent Progress from Layered Assemblies to Layered Nano-architectonics. *Chem. Asian J.* **2019**, *14* (15), 2553–2566.
- (13) Muxika, A.; Etxabide, A.; Uranga, J.; Guerrero, P.; de la Caba, K. Chitosan as a Bioactive Polymer: Processing, Properties and Applications. *Int. J. Biol. Macromol.* **2017**, *105*, 1358–1368.
- (14) Jiang, T.; James, R.; Kumbar, S. G.; Laurencin, C. T. Chapter 5 Chitosan as a Biomaterial: Structure, Properties, and Applications in Tissue Engineering and Drug Delivery. In *Natural and Synthetic Biomedical Polymers*; Elsevier, 2014; pp 91–113.
- (15) Ahsan, S. M.; Thomas, M.; Reddy, K. K.; Sooraparaju, S. G.; Asthana, A.; Bhatnagar, I. Chitosan as Biomaterial in Drug Delivery and Tissue Engineering. *Int. J. Biol. Macromol.* **2018**, *110*, 97–109.
- (16) Sultankulov, B.; Berillo, D.; Sultankulova, K.; Tokay, T.; Saparov, A. Progress in the Development of Chitosan-Based Biomaterials for Tissue Engineering and Regenerative Medicine. *Biomolecules* **2019**, *9* (9), 470.
- (17) Hu, B.; Guo, Y.; Li, H.; Liu, X.; Fu, Y.; Ding, F. Recent Advances in Chitosan-Based Layer-by-Layer Biomaterials and Their Biomedical Applications. *Carbohydr. Polym.* **2021**, *271*, No. 118427.

- (18) Bakhsheshi-Rad, H. R.; Chen, X.; Ismail, A. F.; Aziz, M.; Abdolahi, E.; Mahmoodiyan, F. Improved Antibacterial Properties of an Mg-Zn-Ca Alloy Coated with Chitosan Nanofibers Incorporating Silver Sulfadiazine Multiwall Carbon Nanotubes for Bone Implants. *Polym. Adv. Technol.* **2019**, *30* (5), 1333–1339.
- (19) Jabłoński, P.; Kyzioł, A.; Pawcenis, D.; Pucelik, B.; Hebda, M.; Migdalska, M.; Krawiec, H.; Arruebo, M.; Kyzioł, K. Electrostatic Self-Assembly Approach in the Deposition of Bio-Functional Chitosan-Based Layers Enriched with Caffeic Acid on Ti-6Al-7Nb Alloys by Alternate Immersion. *Biomaterials Advances* **2022**, *136*, No. 212791.
- (20) Bakhsheshi-Rad, H. R.; Hamzah, E.; Ying, W. S.; Razzaghi, M.; Sharif, S.; Ismail, A. F.; Berto, F. Improved Bacteriostatic and Anticorrosion Effects of Polycaprolactone/Chitosan Coated Magnesium via Incorporation of Zinc Oxide. *Materials* **2021**, *14* (8), 1930.
- (21) Lu, B.; Luo, D.; Zhao, A.; Wang, H.; Zhao, Y.; Maitz, M. F.; Yang, P.; Huang, N. PH Responsive Chitosan and Hyaluronic Acid Layer by Layer Film for Drug Delivery Applications. *Prog. Org. Coat.* **2019**, *135*, 240–247.
- (22) Yilmaz, M. D. Layer-by-Layer Hyaluronic Acid/Chitosan Polyelectrolyte Coated Mesoporous Silica Nanoparticles as PH-Responsive Nanocontainers for Optical Bleaching of Cellulose Fabrics. *Carbohydr. Polym.* **2016**, *146*, 174–180.
- (23) Rocha Neto, J. B. M.; Lima, G. G.; Fiamingo, A.; Germiniani, L. G. L.; Taketa, T. B.; Bataglioli, R. A.; da Silveira, G. A. T.; da Silva, J. V. L.; Campana-Filho, S. P.; Oliveira, O. N.; Beppu, M. M. Controlling Antimicrobial Activity and Drug Loading Capacity of Chitosan-Based Layer-by-Layer Films. *Int. J. Biol. Macromol.* **2021**, *172*, 154–161.
- (24) Pérez-Anes, A.; Gargouri, M.; Laure, W.; Van Den Berghe, H.; Courcot, E.; Sobocinski, J.; Tabary, N.; Chai, F.; Blach, J.-F.; Addad, A.; Woisel, P.; Douroumis, D.; Martel, B.; Blanchemain, N.; Lyskawa, J. Bioinspired Titanium Drug Eluting Platforms Based on a Poly- β -Cyclodextrin–Chitosan Layer-by-Layer Self-Assembly Targeting Infections. *ACS Appl. Mater. Interfaces* **2015**, *7* (23), 12882–12893.
- (25) Stankevich, K. S.; Danilenko, N. V.; Gadirov, R. M.; Goreninskii, S. I.; Tverdokhlebov, S. I.; Filimonov, V. D. A New Approach for the Immobilization of Poly(Acrylic) Acid as a Chemically Reactive Cross-Linker on the Surface of Poly(Lactic) Acid-Based Biomaterials. *Materials Science and Engineering: C* **2017**, *71*, 862–869.
- (26) Guzmán, E.; Cavallo, J. A.; Chuliá-Jordán, R.; Gómez, C.; Strumia, M. C.; Ortega, F.; Rubio, R. G. PH-Induced Changes in the Fabrication of Multilayers of Poly(Acrylic Acid) and Chitosan: Fabrication, Properties, and Tests as a Drug Storage and Delivery System. *Langmuir* **2011**, *27* (11), 6836–6845.
- (27) Guzmán, E.; Chuliá-Jordán, R.; Ortega, F.; Rubio, R. G. Influence of the Percentage of Acetylation on the Assembly of LbL Multilayers of Poly(Acrylic Acid) and Chitosan. *Phys. Chem. Chem. Phys.* **2011**, *13* (40), 18200.
- (28) Saracogullari, N.; Gundogdu, D.; Ozdemir, F. N.; Soyer, Y.; Erel-Goktepe, I. The Effect of Polyacid on the Physical and Biological Properties of Chitosan Based Layer-by-Layer Films. *Colloids Surf. A Physicochem Eng. Asp* **2021**, *617*, No. 126313.
- (29) Nalam, P. C.; Lee, H.-S.; Bhatt, N.; Carpick, R. W.; Eckmann, D. M.; Composto, R. J. Nanomechanics of PH-Responsive, Drug-Loaded, Bilayered Polymer Grafts. *ACS Appl. Mater. Interfaces* **2017**, *9* (15), 12936–12948.
- (30) Pokrowiecki, R. The Paradigm Shift for Drug Delivery Systems for Oral and Maxillofacial Implants. *Drug Deliv* **2018**, *25* (1), 1504–1515.
- (31) Shukla, A.; Fuller, R. C.; Hammond, P. T. Design of Multi-Drug Release Coatings Targeting Infection and Inflammation. *J. Controlled Release* **2011**, *155* (2), 159–166.
- (32) Yu, X.; Liao, X.; Chen, H. Antibiotic-Loaded MMT/PLL-Based Coating on the Surface of Endosseous Implants to Suppress Bacterial Infections. *Int. J. Nanomedicine* **2021**, *16*, 2983–2994.
- (33) Bingyun, L.; Fintan, M. T.; Thomas, W.; Malcolm, X.; Racing for the Surface: Antimicrobial and Interface Tissue Engineering; Li, B.; Moriarty, T. F.; Webster, T.; Xing, M., Eds.; Springer International Publishing: Cham, 2020. .
- (34) Gallo, J.; Holinka, M.; Moucha, C. Antibacterial Surface Treatment for Orthopaedic Implants. *Int. J. Mol. Sci.* **2014**, *15* (8), 13849–13880.
- (35) Ritter, B.; Herlyn, P. K. E.; Mittlmeier, T.; Herlyn, A. Preoperative Skin Antisepsis Using Chlorhexidine May Reduce Surgical Wound Infections in Lower Limb Trauma Surgery When Compared to Povidone-Iodine - a Prospective Randomized Trial. *Am. J. Infect Control* **2020**, *48* (2), 167–172.
- (36) Chen, Z.; Mont, M. A. The Utility of Chlorhexidine Cloth Use for the Prevention of Surgical Site Infections in Total Hip Arthroplasty and Surgical as Well as Basic Science Applications. *Orthopedic Clinics of North America* **2023**, *54* (1), 7–22.
- (37) Queiroz, V. M.; Kling, I. C. S.; Eltom, A. E.; Archanjo, B. S.; Prado, M.; Simão, R. A. Corn Starch Films as a Long-Term Drug Delivery System for Chlorhexidine Gluconate. *Materials Science and Engineering: C* **2020**, *112*, No. 110852.
- (38) Matos, A. O.; de Almeida, A. B.; Beline, T.; Tonon, C. C.; Casarin, R. C. V.; Windsor, L. J.; Duarte, S.; Nociti, F. H.; Rangel, E. C.; Gregory, R. L.; Barão, V. A. R. Synthesis of Multifunctional Chlorhexidine-Doped Thin Films for Titanium-Based Implant Materials. *Materials Science and Engineering: C* **2020**, *117*, No. 111289.
- (39) Agarwal, A.; Nelson, T. B.; Kierski, P. R.; Schurr, M. J.; Murphy, C. J.; Czuprynski, C. J.; McAnulty, J. F.; Abbott, N. L. Polymeric Multilayers That Localize the Release of Chlorhexidine from Biologic Wound Dressings. *Biomaterials* **2012**, *33* (28), 6783–6792.
- (40) Harnet, J.-C.; Le Guen, E.; Ball, V.; Tenenbaum, H.; Ogier, J.; Haikel, Y.; Vodouhê, C. Antibacterial Protection of Suture Material by Chlorhexidine-Functionalized Polyelectrolyte Multilayer Films. *J. Mater. Sci. Mater. Med.* **2009**, *20* (1), 185–193.
- (41) Rakhmatullayeva, D.; Ospanova, A.; Bekissanova, Z.; Jumagazyeva, A.; Savdenbekova, B.; Seidulayeva, A.; Sailau, A. Development and Characterization of Antibacterial Coatings on Surgical Sutures Based on Sodium Carboxymethyl Cellulose/Chitosan/Chlorhexidine. *Int. J. Biol. Macromol.* **2023**, *236*, No. 124024.
- (42) Al Thaher, Y.; Abdelghany, S.; Abulateefeh, S. R. PH-Responsive LBL Coated Silica Nanocarriers for Controlled Release of Chlorhexidine. *Colloids Surf. A Physicochem Eng. Asp* **2024**, *680*, No. 132671.
- (43) Olmo, J. A.-D.; Ruiz-Rubio, L.; Pérez-Alvarez, L.; Sáez-Martínez, V.; Vilas-Vilela, J. L. Antibacterial Coatings for Improving the Performance of Biomaterials. *Coatings* **2020**, *10* (2), 139.
- (44) Lin, X.; Yang, M.; Jeong, H.; Chang, M.; Hong, J. Durable Superhydrophilic Coatings Formed for Anti-Biofouling and Oil–Water Separation. *J. Membr. Sci.* **2016**, *506*, 22–30.
- (45) Moran, G.; Ramos-Chagas, G.; Hugelier, S.; Xie, X.; Boudjemaa, R.; Ruckebusch, C.; Sliwa, M.; Darmanin, T.; Gaucher, A.; Prim, D.; Godeau, G.; Amigoni, S.; Guittard, F.; Méallet-Renault, R. Superhydrophobic Polypyrrole Films to Prevent Staphylococcus Aureus and Pseudomonas Aeruginosa Biofilm Adhesion on Surfaces: High Efficiency Deciphered by Fluorescence Microscopy. *Photochemical & Photobiological Sciences* **2018**, *17* (8), 1023–1035.
- (46) Wu, S.; Zhang, B.; Liu, Y.; Suo, X.; Li, H. Influence of Surface Topography on Bacterial Adhesion: A Review (Review). *Biointerphases* **2018**, *13* (6), No. 060801.
- (47) Sugii, M. M.; de Souza Ferreira, F. A.; Müller, K. C.; Filho, U. P. R.; Aguiar, F. H. B. Chapter 5 - Quaternary Ammonium Compound Derivatives for Biomedical Applications. In *Materials for Biomedical Engineering*; Elsevier, 2019; pp 153–175. .
- (48) Makvandi, P.; Jamaledin, R.; Jabbari, M.; Nikfarjam, N.; Borzacchiello, A. Antibacterial Quaternary Ammonium Compounds in Dental Materials: A Systematic Review. *Dental Materials* **2018**, *34* (6), 851–867.
- (49) Bucolo, C.; Gozzo, L.; Longo, L.; Mansueto, S.; Vitale, D. C.; Drago, F. Long-Term Efficacy and Safety Profile of Multiple Injections of Intravitreal Dexamethasone Implant to Manage Diabetic

Macular Edema: A Systematic Review of Real-World Studies. *J. Pharmacol. Sci.* **2018**, *138* (4), 219–232.

(50) Choi, D.; Heo, J.; Park, J. H.; Jo, Y.; Jeong, H.; Chang, M.; Choi, J.; Hong, J. Nano-Film Coatings onto Collagen Hydrogels with Desired Drug Release. *Journal of Industrial and Engineering Chemistry* **2016**, *36*, 326–333.

(51) Zander, Z. K.; Becker, M. L. Antimicrobial and Antifouling Strategies for Polymeric Medical Devices. *ACS Macro Lett.* **2018**, *7* (1), 16–25.

(52) Quinn, J.; McFadden, R.; Chan, C.-W.; Carson, L. Titanium for Orthopedic Applications: An Overview of Surface Modification to Improve Biocompatibility and Prevent Bacterial Biofilm Formation. *iScience* **2020**, *23* (11), No. 101745.

(53) Akay, S.; Yaghmur, A. Recent Advances in Antibacterial Coatings to Combat Orthopedic Implant-Associated Infections. *Molecules* **2024**, *29* (5), 1172.

(54) Jing, Z.; Zhang, T.; Xiu, P.; Cai, H.; Wei, Q.; Fan, D.; Lin, X.; Song, C.; Liu, Z. Functionalization of 3D-Printed Titanium Alloy Orthopedic Implants: A Literature Review. *Biomedical Materials* **2020**, *15* (5), No. 052003.

(55) Shree, P.; Singh, C. K.; Sodhi, K. K.; Surya, J. N.; Singh, D. K. Biofilms: Understanding the Structure and Contribution towards Bacterial Resistance in Antibiotics. *Medicine in Microecology* **2023**, *16*, No. 100084.

(56) Ruan, H.; Aulova, A.; Ghai, V.; Pandit, S.; Lovmar, M.; Mijakovic, I.; Kádár, R. Polysaccharide-Based Antibacterial Coating Technologies. *Acta Biomater* **2023**, *168*, 42–77.

(57) Nazarov, D.; Zemtsova, E.; Solokhin, A.; Valiev, R.; Smirnov, V. Modification of the Surface Topography and Composition of Ultrafine and Coarse Grained Titanium by Chemical Etching. *Nanomaterials* **2017**, *7* (1), 15.

(58) Mukaddam, K.; Astasov-Frauenhoffer, M.; Fasler-Kan, E.; Ruggiero, S.; Alhawasli, F.; Kisiel, M.; Meyer, E.; Köser, J.; Bornstein, M. M.; Wagner, R. S.; Kühn, S. Piranha-Etched Titanium Nanostructure Reduces Biofilm Formation in Vitro. *Clin Oral Investig* **2023**, *27* (10), 6187–6197.

(59) Wang, Z.; Wang, J.; Wu, R.; Wei, J. Construction of Functional Surfaces for Dental Implants to Enhance Osseointegration. *Front. Bioeng. Biotechnol.* **2023**, *11*, No. 1320307.

(60) Jacobs, T. W.; Dillon, J. T.; Cohen, D. J.; Boyan, B. D.; Schwartz, Z. Different Methods to Modify the Hydrophilicity of Titanium Implants with Biomimetic Surface Topography to Induce Variable Responses in Bone Marrow Stromal Cells. *Biomimetics* **2024**, *9* (4), 227.

(61) Bieker, P.; Schönhoff, M. Linear and Exponential Growth Regimes of Multilayers of Weak Polyelectrolytes in Dependence on PH. *Macromolecules* **2010**, *43* (11), 5052–5059.

(62) Yılmaz Aykut, D.; Yolaçan, Ö.; Deligöz, H. PH Stimuli Drug Loading/Release Platforms from LbL Single/Blend Films: QCM-D and in-Vitro Studies. *Colloids Surf. A Physicochem Eng. Asp* **2020**, *602*, No. 125113.

(63) Shiratori, S. S.; Rubner, M. F. PH-Dependent Thickness Behavior of Sequentially Adsorbed Layers of Weak Polyelectrolytes. *Macromolecules* **2000**, *33* (11), 4213–4219.

(64) Cagli, E.; Ugur, E.; Ulsan, S.; Banerjee, S.; Erel-Goktepe, I. Effect of Side Chain Variation on Surface and Biological Properties of Poly(2-Alkyl-2-Oxazoline) Multilayers. *Eur. Polym. J.* **2019**, *114*, 452–463.

(65) Potaś, J.; Winnicka, K. The Potential of Polyelectrolyte Multilayer Films as Drug Delivery Materials. *Int. J. Mol. Sci.* **2022**, *23* (7), 3496.

(66) Mateos-Maroto, A.; Abelenda-Núñez, I.; Ortega, F.; Rubio, R. G.; Guzmán, E. Polyelectrolyte Multilayers on Soft Colloidal Nanosurfaces: A New Life for the Layer-By-Layer Method. *Polymers (Basel)* **2021**, *13* (8), 1221.

(67) Criado-Gonzalez, M.; Fernandez-Gutierrez, M.; San Roman, J.; Mijangos, C.; Hernández, R. Local and Controlled Release of Tamoxifen from Multi (Layer-by-Layer) Alginate/Chitosan Complex Systems. *Carbohydr. Polym.* **2019**, *206*, 428–434.

(68) Pilicheva, B.; Uzunova, Y.; Bodurov, I.; Viraneva, A.; Exner, G.; Sotirov, S.; Yovcheva, T.; Marudova, M. Layer-by-Layer Self-Assembly Films for Buccal Drug Delivery: The Effect of Polymer Cross-Linking. *J. Drug Deliv. Sci. Technol.* **2020**, *59*, No. 101897.

(69) Potaś, J.; Szymańska, E.; Wróblewska, M.; Kurowska, I.; Maciejczyk, M.; Basa, A.; Wolska, E.; Wilczewska, A. Z.; Winnicka, K. Multilayer Films Based on Chitosan/Pectin Polyelectrolyte Complexes as Novel Platforms for Buccal Administration of Clotrimazole. *Pharmaceutics* **2021**, *13* (10), 1588.

(70) de Villiers, M. M.; Otto, D. P.; Strydom, S. J.; Lvov, Y. M. Introduction to Nanocoatings Produced by Layer-by-Layer (LbL) Self-Assembly. *Adv. Drug Deliv. Rev.* **2011**, *63* (9), 701–715.

(71) de Avila, E. D.; Castro, A. G. B.; Tagit, O.; Krom, B. P.; Löwik, D.; van Well, A. A.; Bannenberg, L. J.; Vergani, C. E.; van den Beucken, J. J. P. Anti-Bacterial Efficacy via Drug-Delivery System from Layer-by-Layer Coating for Percutaneous Dental Implant Components. *Appl. Surf. Sci.* **2019**, *488*, 194–204.

(72) Shen, Y.; Stojicic, S.; Haapasalo, M. Antimicrobial Efficacy of Chlorhexidine against Bacteria in Biofilms at Different Stages of Development. *J. Endod.* **2011**, *37* (5), 657–661.

(73) Srisang, S.; Nasongkla, N. Layer-by-Layer Dip Coating of Foley Urinary Catheters by Chlorhexidine-Loaded Micelles. *J. Drug Deliv. Sci. Technol.* **2019**, *49*, 235–242.